

Static Electric Dipole Polarizabilities of Na Clusters

S. Kümmel¹, T. Berkus², P.-G. Reinhard², and M. Brack¹

¹ Institute for Theoretical Physics, University of Regensburg, D-93040 Regensburg, Germany

² Institute for Theoretical Physics, University of Erlangen, D-91077 Erlangen, Germany

Received: date / Revised version: date

Abstract. The static electric dipole polarizability of Na_N clusters with even N has been calculated in a collective, axially averaged and a three-dimensional, finite-field approach for $2 \leq N \leq 20$, including the ionic structure of the clusters. The validity of a collective model for the static response of small systems is demonstrated. Our density functional calculations verify the trends and fine structure seen in a recent experiment. A pseudopotential that reproduces the experimental bulk bond length and atomic energy levels leads to a substantial increase in the calculated polarizabilities, in better agreement with experiment. We relate remaining differences in the magnitude of the theoretical and experimental polarizabilities to the finite temperature present in the experiments.

PACS. 36.40.-c Atomic and molecular clusters – 31.15.E Density functional theory in atomic and molecular physics – 33.15.Kr Properties of molecules, electric polarizability

1 Introduction

The measurement of the static electric polarizability of sodium clusters [1] and its interpretation in terms of the jellium model [2] was one of the triggers for the research activities that today form the field of modern metal cluster physics. The first theoretical studies were followed by several others with different methods and aims: density functional calculations using pseudopotentials [3, 4] or taking all electrons into account [5] aimed at a quantitative description of the experimentally observed effects, semi-classical approaches [6] focused on size-dependent trends, and the static electric polarizability served to test and compare theoretical concepts [7, 8, 9]. Recently, the field received new inspiration from a second experimental determination of the static polarizability of small, uncharged Na clusters [10].

Whereas a qualitative understanding of the experiments can be obtained with relatively simple models, a quantitative theoretical determination of the polarizability requires knowledge of the ionic and electronic configurations of the clusters. Great effort has been devoted in the past to determine these [4, 11, 12, 13]. However, taking all ionic and electronic degrees of freedom into account in a three-dimensional calculation is a task of considerable complexity. Therefore, most of these studies were restricted to clusters with not more than nine atoms. To reduce the computational expense, approximations for including ionic effects were developed [14, 15, 16, 17, 18, 19]. A second problem, however, is the great number of closely lying isomers that are found in sodium clusters. This effect is especially pronounced when stabilization of an overall

shape through electronic shell effects is weak, i.e. for the “soft” clusters that are found between filled shells. In the present work we present calculations for the static electric polarizability that include the ionic structure in a realistic way. We take into account a great number of isomers for clusters with up to 20 atoms, especially for the soft clusters that fill the second electronic shell. The theoretical concepts that we used in this study are introduced in section 2, where we also discuss the relevant cluster structures. In section 3 we present our results and compare with other calculations and experimental work. Our conclusions are summarized in section 4.

2 Theoretical concepts

The starting point for the theoretical determination of the polarizability of a cluster is the calculation of the ionic and electronic configuration of the ground-state and close lying isomers. In the present work, this was done in two steps. First, we calculated low-energy ionic geometries for a wide range of cluster sizes with an improved version [19] of the “Cylindrically Averaged Pseudopotential Scheme” (CAPS) [18]. In CAPS the ions are treated fully three-dimensionally, but the valence electrons are restricted to axial symmetry. The cluster ground state is found by simultaneously minimizing the energy functional with respect to the set of ionic positions (simulated annealing) and the valence-electron density. For the exchange and correlation energy we used the local-density approximation (LDA) functional of Perdew and Wang [20], and for the pseudopotential we employed the recently developed

phenomenological smooth-core potential that reproduces low temperature bulk and atomic properties [19]. Detailed comparisons with *ab initio* calculations have shown [19] that CAPS predicts ionic geometries of sodium clusters rather accurately since truly triaxial deformations are rare. Furthermore, in a second step we performed fully three-dimensional (3D) Kohn-Sham (KS) calculations to check the ordering of isomers and to calculate polarizabilities without axial restriction on the electrons, and also included configurations from 3D geometry optimizations into our analysis as discussed below.

Fig. 1 schematically depicts the most important ionic geometries for neutral clusters with even electron numbers between 2 and 20. (We have calculated the polarizabilities also for many further and higher isomers which, however, are not shown in Fig. 1 for the sake of clarity. They were omitted from the discussion since they do not lead to qualitatively different results.) For the small clus-

ters Na_2 , Na_4 and Na_6 , many other theoretical predictions have been made [3, 4, 10, 12, 13], and our geometries are in perfect agreement with them. In addition, due to the construction of the pseudopotential [19], the bond lengths are close to the experimental ones, as e.g. seen in the dimer, where our calculated bond length is $5.78a_0$ and the experimental one [21] is $5.82a_0$. For Na_8 and Na_{10} , our results are in agreement with 3D density functional calculations [3, 4, 13]. For Na_{12} , we do not know of any *ab initio* calculations. Therefore, besides two low-energy configurations from CAPS [(a) and (b)], we also included a locally re-optimized low-energy geometry from a 3D, Hückel model calculation [15] in our analysis (c). Our 3D calculations confirm our CAPS results and find structures (a) and (b) quasi degenerate with a difference in total energy of 0.05 eV, whereas structure (c) is higher by 0.4 eV. Two of the three geometries considered for Na_{14} [(b) and (c)] were also found very similar in 3D Hückel model calculations [15, 17], and both CAPS and the 3D KS calculations find all of them very close in energy. For Na_{16} , we find as the CAPS-ground state structure (a), and in our 3D calculations structure (b) is quasi degenerate with (a), whereas structures (c) and (d) are higher by 0.08 eV and 0.5 eV. Due to their very different overall shapes, these isomers span a range of what can be expected for the polarizability. For Na_{18} and Na_{20} , our structures are again in close agreement with the 3D density functional calculation of [13], and all three structures are quasi degenerate.

The static electric polarizability was calculated in two different ways. The first is based on a collective description of electronic excitations. It uses the well known equality

$$\alpha = 2m_{-1}, \quad (1)$$

which relates the negative first moment

$$m_{-1}(\mathbf{Q}) = \int_0^\infty E^{-1} S_{\mathbf{Q}}(E) dE = \sum_{\nu} (\hbar\omega_{\nu})^{-1} |\langle \nu | \mathbf{Q} | 0 \rangle|^2 \quad (2)$$

of the strength function

$$S_{\mathbf{Q}}(E) = \sum_{\nu} |\langle \nu | \mathbf{Q} | 0 \rangle|^2 \delta(E_{\nu} - E_0 - E), \quad (3)$$

to the static electric polarizability α in the direction specified by the external (dipole) excitation operator \mathbf{Q} .

In the evaluation of the strength function, the excited states $|\nu\rangle$ are identified with collective excitations. A discussion of this approach can be found in [22]. The collective calculations were carried out using the cylindrically averaged densities and the “clamped nuclei approximation” [4], *i.e.* the ionic positions were taken to be the same with and without the dipole field. We have also checked this widely used approximation in the context of our studies and find it well justified, as discussed below.

The static polarizability can also be calculated directly from the derivative of the induced dipole moment $\boldsymbol{\mu}$ in the presence of an external electric dipole field \mathbf{F} (“finite field method”):

$$\alpha_{ij} = \frac{\mu_j(+F_i) - \mu_j(-F_i)}{2F_i}, \quad i, j = x, y, z, \quad (4)$$

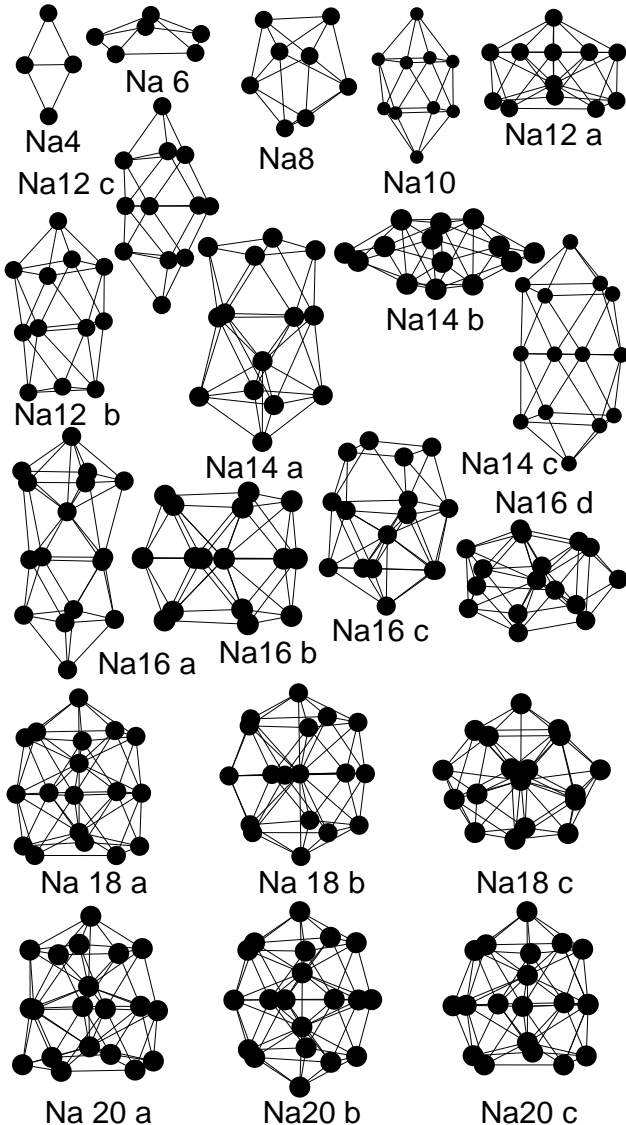


Fig. 1. Cluster structures Na_4 to Na_{20} . See text for discussion.

where

$$\mu_j(\mathbf{F}) = -e \int r_j n(\mathbf{r}, \mathbf{F}) d^3r + eZ \sum_{\mathbf{R}} R_j \quad (5)$$

for ions with valence Z . Here one has to make sure that the numerically applied finite dipole field \mathbf{F} is small enough to be in the regime of linear response, but that it is on the other hand large enough to give a numerically stable signal. We have carefully checked this and found that the used field strengths between $0.00001e/a_0^2$ and $0.0005e/a_0^2$ meet both requirements. Applied to the axial calculations, this approach allows to obtain the polarizability in the z -direction. By employing this method with the 3D KS calculations we have checked the influences of the axial averaging and the collective model on the polarizability and found that the z -polarizabilities from the axial and the 3D finite-field calculations agree within 1% on the average for the low-energy isomers. This shows that the axial averaging is a good approximation for the clusters discussed here. The performance of the collective model will be discussed below in Section 3.1. The orientation of our coordinate system was chosen such that the z -axis is in that principal direction of the tensor of inertia in which it deviates most from its average value. The average static electric polarizability

$$\bar{\alpha} := \frac{1}{3} \text{tr}(\alpha) \quad (6)$$

of course is independent of the choice of coordinate system.

3 Results

3.1 Comparison of different theoretical results

Since all density functional calculations that we know of agree on the geometry of the smallest sodium clusters, these clusters can serve as test cases to compare different theoretical approaches. In Table 1 we have listed the averaged static dipole polarizability as obtained in different calculations, together with the value obtained in the recent experiment of Rayane *et al.* [10]. All calculations reproduce the experimental trend and give the correct overall magnitude. But also, all calculations underestimate the polarizability. The magnitude of this underestimation, however, varies considerably for the different approaches. Whereas our results are closest to the experiment and close to the theoretical ones of Ref. [10], with the largest difference to the experiment being 8 % for Na_8 , a difference of 27 % is found for this cluster in the calculation based on the *ab initio* Bachelet, Hamann, Schlüter (BHS) Pseudopotential [4]. A good part of this difference can be explained by comparing the bond lengths of the clusters. The BHS pseudopotential considerably underestimates the bond lengths [4], leading to a higher electron density and a lower polarizability. Our empirical smooth-core pseudopotential, on the other hand, was constructed to reproduce the experimental low-temperature bulk bond

length (together with the compressibility and the atomic $3s$ -level) when used with the LDA, and correspondingly results in a higher polarizability, in better agreement with experiment. It is further interesting to note that also the polarizabilities calculated with the empirical Bardsley potential [3], which was constructed to reproduce atomic energy levels, are noticeably higher than the BHS-based values. This shows that the cluster polarizability is also sensitive to atomic energy levels, and the fact that our values are closest to the experiment thus is a natural consequence of the combination of correct atomic energy levels and bond lengths.

Table 1. Averaged static electric polarizability of small sodium clusters in \AA^3 . Brd: density functional (DF) calculation with empirical non-local Bardsley pseudopotential [3]. BHS: DF calculation with *ab initio* non-local Bachelet, Hamann, Schlüter pseudopotential [4]. All el.: all-electron DF calculation including gradient corrections to the exchange-correlation functional [5]. TM: DF calculation with Troullier-Martins non-local pseudopotential [9]. GAUSS.: DF calculation based on the GAUSSIAN94 program with SU basis set [10]. Present: present work, values from three-dimensional approach. ExpR: recent experiment [10].

	Brd.	BHS	All el.	TM	GAUSS.	Present	ExpR
Na_2	37.7	33.1	35.9	36.2	38.2	37.0	39.3
Na_4	76.3	67.1	71.4	77.2	78.4	78.7	83.8
Na_6	100.3	89.4	94.8	not	104.4	107.3	111.8
Na_8	111.7	97.0	not	117.6	119.2	123.0	133.6

From comparison with the calculations that went beyond the LDA [5,10], it however becomes clear that the empirical pseudopotentials by construction "compensate" some of the errors that are a consequence of the use of the LDA. Therefore, it would be dangerous to argue that the inclusion of gradient corrections, which have been shown to increase the polarizability, could bring our calculated values in agreement with experiment: going beyond the LDA but keeping the empirical LDA pseudopotentials could lead to a double counting of effects. We therefore conclude that, on the one hand, a considerable part of the earlier observed differences between theoretical and experimental polarizabilities can be attributed to effects associated with errors in the bond lengths or atomic energy levels, but on the other hand, further effects must contribute to the underestimation with respect to experiment. We will come back to this second point below.

In Table 2 we have listed the polarizabilities of Na_2 to Na_{20} for the geometries shown in Fig. 1. The left half gives the polarizability as computed from the 3D electron density with the finite-field method, and the right half lists the values obtained in the axially averaged collective approach. For the clusters up to Na_8 , the two methods agree well and the differences for the averaged polarizabilities are less than 1% for Na_2 and Na_8 , and 3% for Na_4 and Na_6 . This shows that the collective description is rather accurate, which is remarkable if one recalls that we are

dealing with only very few electrons. Beyond Na_8 , the differences are 6 % on the average, which is still fair, but obviously higher. This looks counter-intuitive at first sight, because the collective description should become better for larger systems. However, for $N > 8$ there comes an increasing number of particle-hole states close to the Mie plasmon resonance [22], leading to increasing fragmentation of the collective strength. m_{-1} and thus α is sensitive to energetically low-lying excitations since their energies enter in the denominator in Eq. 2, and this can lead to an underestimation of the polarizability.

Table 2. Static electric polarizability in \AA^3 for the cluster geometries of Fig. 1. Left half: three-dimensional, finite field calculation. Right half: cylindrically averaged, collective calculation.

	3D, finite field				cyl., coll. mod.		
	α_x	α_y	α_z	$\bar{\alpha}$	α_ρ	α_z	$\bar{\alpha}$
Na_2	29.9	29.9	51.3	37.0	30.2	51.5	37.3
Na_4	47.0	59.0	130.1	78.7	53.7	122.6	76.7
Na_6	129.8	129.8	62.2	107.3	124.9	62.1	103.9
Na_8	118.1	118.5	132.3	123.0	117.5	131.4	122.1
Na_{10}	126.3	126.3	219.3	157.3	125.3	194.5	148.4
Na_{12a}	213.4	213.4	155.7	194.2	199.5	143.6	180.9
Na_{12b}	156.5	158.6	261.1	192.1	151.3	234.7	179.1
Na_{12c}	158.6	145.1	285.3	196.3	148.7	252.0	183.1
Na_{14a}	183.5	183.5	278.9	215.3	177.5	251.7	202.2
Na_{14b}	271.3	273.9	137.8	227.7	264.2	132.7	220.4
Na_{14c}	175.2	179.3	291.3	215.3	171.1	262.5	201.6
Na_{16a}	193.5	193.5	394.5	260.5	190.3	318.4	233.0
Na_{16b}	235.2	235.2	231.5	234.0	227.3	220.3	225.0
Na_{16c}	212.5	213.4	272.2	232.7	206.0	255.1	222.4
Na_{16d}	272.2	260.8	239.3	239.3	260.6	185.1	235.4
Na_{18a}	260.3	262.5	291.3	271.4	236.4	266.7	246.5
Na_{18b}	251.8	250.7	283.8	262.1	232.6	253.4	239.5
Na_{18c}	281.6	280.5	250.7	270.9	255.9	227.7	246.5
Na_{20a}	285.7	284.5	309.4	293.2	269.7	279.7	273.0
Na_{20b}	275.0	275.0	311.8	287.3	261.8	282.9	268.8
Na_{20c}	267.9	271.5	295.2	278.2	283.2	280.3	282.2

Comparing the polarizabilities of clusters with the same number of electrons but different geometries shows the influence of the overall shape of the cluster. For Na_{14} , e.g., isomers (a) and (c) have a valence electron density which is close to prolate, whereas (b) has a more oblate one. The averaged polarizability for the two prolate isomers is equal, although their ionic geometries differ. The oblate isomer, however, has a noticeably higher averaged polarizability. This is what one expects, because for oblate clusters there are two principal directions with a low and one with a high polarizability, whereas for prolate clusters the reverse is true. The fact that different ionic geometries can lead to very similar averaged polarizabilities is also seen for Na_{12} . It thus becomes clear that contrary to what was believed earlier [3] one cannot necessarily distinguish between details in the ionic configuration by comparing theoretical values to experimental data that measure the averaged polarizability.

3.2 Comparison with experiments

Fig. 2 shows $\bar{\alpha}$ for our ground state structures as obtained in the axial, collective approach and the 3D finite-field calculations, in comparison to the two available sets of experimental data. The absolute values for the experiments were calculated from the measured relative values with an atomic polarizability of 23.6\AA^3 [10]. To guide the eye, the polarizabilities from each set of data are connected by lines. Both experiments and the theoretical data show that, overall, the polarizability increases with increasing cluster size. The polarizability from the axial collective model qualitatively shows the same behavior as the one from the 3D finite field calculation. Comparison of the

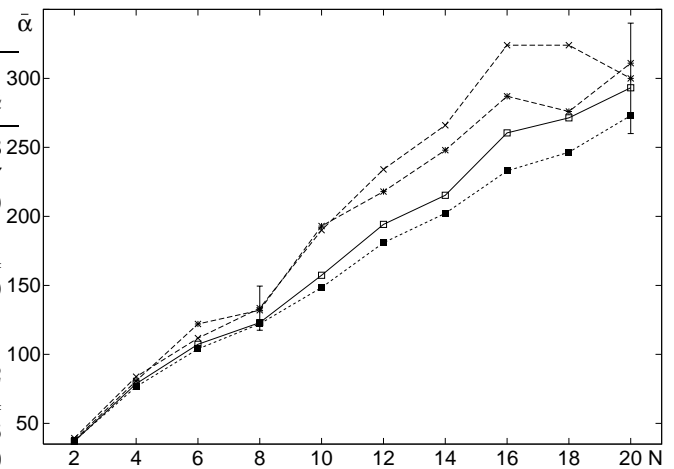


Fig. 2. Static electric dipole polarizability in \AA^3 versus number of electrons. Crosses with thin, long dashed line: experiment of Rayane *et al.* [10]; stars with strong, long dashed line: experiment of Knight *et al.* [1]; open squares with full line: present work, three-dimensional finite-field calculation for lowest isomer; filled squares with short dashed line: present work, axially averaged collective calculation for lowest isomer. See text for discussion of error bars.

3D values with the experimental data shows that for the smallest clusters, the theoretical and experimental values agree as discussed before, and the values obtained in the two experiments are comparable up to Na_{10} . Beyond Na_{10} , the discrepancies between the two experiments become larger, and also the differences between theoretical and experimental polarizabilities increase. For Na_{12} , Na_{14} , Na_{16} and Na_{18} the experiment of Knight *et al.* gives lower values than the experiment of Rayane *et al.*, and the calculated averaged polarizability is lower than both experiments for Na_{12} , Na_{14} , and Na_{16} . For Na_{18} the finite-field value obtained for our ground-state structure matches the value measured by Knight *et al.*, and for Na_{20} , our ground-state polarizability is very close to the measurement of Rayane *et al.* In this discussion one must keep in mind, however, that the experimental uncertainty is about $\pm 2\text{\AA}^3$ per atom [10], i.e. the uncertainty in the absolute value increases with the cluster size, as indicated by the error bars in Fig. 2. Comparisons are made easier if the linear

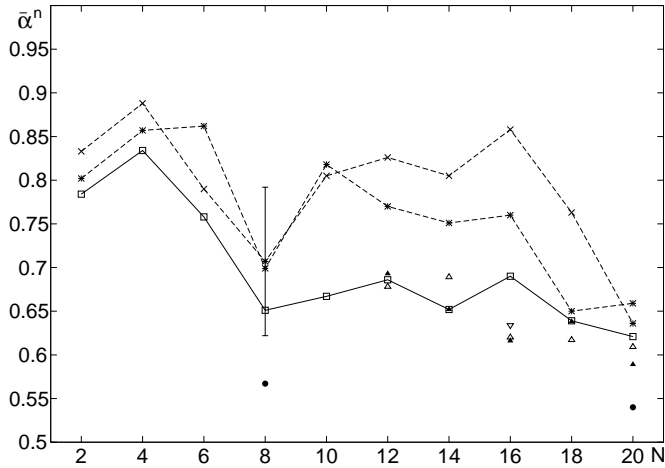


Fig. 3. Normalized static electric dipole polarizability. Crosses with thin dashed line: experiment of Rayane *et al.* [10]; stars with strong dashed line: experiment of Knight *et al.* [1]; squares with full line: present work, three-dimensional finite-field calculation for lowest isomer; open triangle, filled triangle and upside-down triangle: second, third and fourth isomer, respectively; filled circles: Jellium results from [2, 8]. See text for discussion.

growth in $\bar{\alpha}$ is scaled away. Therefore, one should rather look at the normalized polarizability

$$\bar{\alpha}^n := \frac{\bar{\alpha}}{N\alpha_{\text{atom}}}, \quad (7)$$

which is shown in Fig. 3, because it allows to identify trends and details more clearly.

From Fig. 3 it becomes clear that for Na_2 to Na_8 , the trend seen in the two experiments is similar up to one exception: For Na_6 , the experiment of Rayane *et al.* predicts a noticeably smaller value than the one by Knight *et al.* Comparison with our theoretical data shows that, although the values of the older experiment are closer to the theory with respect to magnitude for Na_2 , Na_4 and Na_8 , the trend that our data show corresponds clearly to the one seen in the new experiment since the two curves are parallel. Going from Na_8 to Na_{10} , both experiments predict a steep rise in the polarizability. This rise due to the shell closing at Na_8 is also seen in the theoretical data, but it is less pronounced than in the experiments (as we will discuss below). For Na_{12} , a higher $\bar{\alpha}^n$ than for Na_{10} is predicted by the data of Rayane, whereas the reverse ordering is seen in the data of Knight *et al.* Again, our calculations support the finding of the new experiment, and all isomers lead to similar $\bar{\alpha}^n$. For Na_{14} , both experiments show a decrease. Our prolate ground state and isomer reproduce this trend. That it is the prolate structures that fit to the experiment is consistent with the *ab initio* molecular dynamics calculations of Häkkinen *et al.* [23]. The next step to Na_{16} again reveals a slight difference between the two experiments: both predict an increase compared to Na_{14} , but whereas the older experiment sees $\bar{\alpha}^n$ smaller for Na_{16} than for Na_{12} , the new experiment shows the opposite ordering. Once more, our ground state

structure leads to a polarizability that follows the trend of the new experiment. (The other isomers, however, lead to smaller polarizabilities, and an explanation for the difference between the experiments thus might be that different ensembles of isomers were populated due to slightly different experimental conditions.) Going to Na_{18} leads to a decrease in the polarizability in both experiments. Our calculation shows this decrease, which is a manifestation of the nearby shell closing. But whereas the old experiment actually sees the shell closing at Na_{18} and an increase in the polarizability for Na_{20} , the new experiment and our data find an absolute minimum at Na_{20} .

A comparison with the polarizability obtained in the spherical jellium model [2, 8] for Na_8 and Na_{20} , also indicated in Fig. 3, shows the improvement that is brought about by the inclusion of the ionic structure.

3.3 Discussion

As just discussed, our calculations reproduce the fine structure seen in the new experiment. However, there is no obvious explanation for why the results of the two experiments differ [24]. Also, there is a characteristic change in the magnitude of the difference between our theoretical results and the experimental values of Rayane *et al.*: whereas the calculated values for Na_2 to Na_8 and Na_{20} on the average differ only by 5 % from the new experiment, the open-shell clusters from Na_{10} to Na_{18} show 18 % difference for the ground state. The increase in polarizability when going from Na_8 to Na_{10} is considerably underestimated, whereas the following steps in the normalized polarizability are nearly reproduced correctly, i.e. it looks as if the theoretical curve for Na_{10} to Na_{18} should be shifted upwards by a constant. A first suspicion might be that this “offset” could be due to the use of CAPS in the geometry optimization. But it should be noted that the step occurs at Na_{10} , and that also Na_{14} and Na_{18} are off by the same amount. Since the low-energy structures of these clusters are well established, as discussed in Section 2, and since also the geometry for Na_{12} from the 3D calculation does not lead to qualitatively different results, we can conclude that the differences are not due to limits in the geometry optimization with CAPS. Also, the neglect of the relaxation of the nuclei in the presence of the electric dipole field has been investigated earlier [4] for the small clusters and was shown to be a good approximation. We have counter checked this result for the test case Na_{10} and find corrections of less than 1%.

An obvious limitation of our approach is the neglect of the core polarization. However, the all-electron calculations of Guan *et al.* [5] treat the core electrons explicitly and do not lead to better agreement with experiment, as discussed in Section 3.1. From this, one already can conclude that core polarization cannot account for all of the observed differences. Its effect can be estimated from the polarizability of the sodium cation. Different measurements [25] find values between 0.179 \AA^3 and 0.41 \AA^3 , leading to corrections of - roughly - 1-2 % in $\bar{\alpha}^n$. Since the core polarizability leads to a shift in $\bar{\alpha}^n$ that is the same for all

cluster sizes, it contributes to the difference that is also seen for the smallest clusters, but it cannot explain the jump in the difference seen at Na_{10} .

Another principal limitation of our approach is the use of the LDA. As, e.g., discussed in [5], the LDA can affect the polarizability in different and opposing ways. On the one hand it may lead to an overscreening and thus an underestimation of the polarizability, and early calculations within the spherical jellium model reported that indeed the static polarizability was increased if one went beyond LDA using self-interaction corrections [7]. On the other hand, self-interaction corrections can lead to more negative single particle energies and thus to smaller polarizabilities [5], and Refs. [8] and [26] give examples where the overall effect of self-interaction corrections on the optic response is very small. One cannot directly conclude from the jellium results to our ionic structure calculations, because the sharp edge of the steep-wall jellium model can qualitatively lead to differences. But in any case it is highly implausible that the LDA affects the clusters from Na_{10} to Na_{18} much stronger than the other ones, and it should also be kept in mind that the worst indirect effects of the LDA as, e.g., underestimation of bond lengths, are compensated by using our phenomenological pseudopotential.

One might also ponder about possible uncertainties in the experimental determination of the polarizabilities. A considerable underestimation could be explained if one assumes that while passing through the deflecting field, the clusters are oriented such that one always measures the highest component of the polarizability. In that case, we would not have to compare the averaged value to the experiment, but the highest one. One could imagine that the cluster's rotation be damped, since angular momentum conservation is broken by the external field and the energy thus could be transferred from the rotation to internal degrees of freedom (vibrations). The time scale of this energy transfer is not known, but since the clusters are spending about 10^{-4} s in the deflecting field region, it seems unlikely that there should be no coupling over such a long time. One could further argue that for statistical reasons it is less likely that a larger cluster will lose its orientation again through random-like thermal motion of its constituent ions than a smaller cluster. However, the maximal energy difference between different orientations is very small, for Na_{10} , e.g., it is $0.3\text{K } k_B$ for the typical field strength applied in the experiment [1]. Thus, thermal fluctuations can be expected to wipe out any orientation.

From another point of view, however, the finite temperature explains a good part of the differences that our calculations (and other calculations for the small clusters) show in comparison to the experimental data. Whereas our calculations were done for $T=0$, the supersonic nozzle expansion used in the experiment produces clusters with an internal energy distribution corresponding to about 400 - 600 K [27,28]. An estimate based on the thermal expansion coefficient of bulk sodium leads to an increase in the bond lengths of about 3 %, and a detailed finite-temperature CAPS calculation [29] for Na_{11}^+ at 400 K also shows a bond length increase of 3 %. This will only be a

lower limit, since in neutral clusters one can expect a larger expansion than in the bulk due to the large surface, and also a larger expansion than for charged clusters. Thus, to get an estimate for the lower limit of what can be expected from thermal expansion, we have scaled the cluster coordinates by 3 % and again calculated the polarizabilities, finding an increase of about 3 % for the planar and 5 % for three-dimensional structures. This finding is consistent with the results of Guan *et al.* Together with the corrections that are to be expected from the core polarizability, this brings our results for the small and the closed shell clusters in quantitative agreement with the experimental data.

4 Summary and Conclusion

We have presented calculations for the static electric dipole polarizability for sodium clusters with atom numbers between 2 and 20, covering several low-energy structures for each cluster size beyond Na_{10} . By comparing our results to previous calculations for the smallest clusters, we have shown that a pseudopotential which correctly reproduces atomic and bulk properties also improves the static response considerably. We have shown that a collective model for the excited states of sodium clusters, whose validity for the dynamical response was established previously, works reasonably also for the static response in realistic systems. Over the whole range of cluster sizes studied in the present work, we confirm the fine structure seen in a recent experiment. By comparing the calculated averaged polarizability of different isomers for the same cluster size to the measured polarizability, we showed that completely different ionic geometries can lead to very similar averaged polarizabilities. By considering higher isomers we furthermore took a first step to take into account the finite temperature present in the experiment. Our results show that for the open shell clusters from Na_{10} to Na_{18} , also higher lying isomers do not close the remaining gap between theory and experiment. This shows that it is a worthwhile task for future studies to investigate the influence of finite temperatures on these “soft” clusters explicitly. For Na_2 to Na_8 and Na_{20} , we showed that quantitative agreement is already obtained when the effects of thermal expansion and the core polarizability are taken into account.

One of us (S. Kümmel) thanks K. Hansen for several clarifying discussions concerning the experimental temperatures and time-scales, especially with respect to the “orientation question”, and the Deutsche Forschungsgemeinschaft for financial support.

References

1. W. D. Knight, K. Clemenger, W. A. de Heer, and W. A. Saunders, Phys. Rev. B **31**, (1985) 2539.
2. W. Ekardt, Phys. Rev. Lett. **52**, (1984) 1925.

3. I. Moullet, J. L. Martins, F. Reuse, and J. Buttet, *Phys. Rev. Lett.* **65**, (1990) 476.
4. I. Moullet, J. L. Martins, F. Reuse, and J. Buttet, *Phys. Rev. B* **42**, (1990) 11589.
5. J. Guan, M. E. Casida, A. M. Köster, and D. R. Salahub, *Phys. Rev. B* **52**, (1995) 2184.
6. M. Brack, *Phys. Rev. B* **39**, (1989) 3533.
7. J. M. Pacheco and W. Ekardt, *Z. Phys. D* **24**, (1992) 65.
8. M. Madjet, C. Guet, and W. R. Johnson, *Phys. Rev. B* **51**, (1995) 1327.
9. I. Vasiliev, S. Ögüt, and J. R. Chelikowsky, *Phys. Rev. Lett.* **82**, (1999) 1919.
10. D. Rayane, A. R. Allouche, E. Benichou, R. Antoine, M. Aubert-Frecon, Ph. Dugourd, M. Broyer, C. Ristori, F. Chandezon, B. A. Huber, and C. Guet, Contribution to ISSPIC 9, Lausanne, 1998, to appear in *Eur. Phys. J. D* **9**.
11. J. L. Martins, J. Buttet, and R. Car, *Phys. Rev. B* **31**, (1985) 1804.
12. V. Bonačić-Koutecký, P. Fantucci, and J. Koutecký, *Chem. Rev. B* **91**, (1991) 1035.
13. U. Röthlisberger and W. Andreoni, *J. Chem. Phys.* **94**, (1991) 8129.
14. M. P. Iñiguez, M. J. Lopez, J. A. Alonso, and J. M. Soler, *Z. Phys. D* **11**, (1989) 163.
15. R. Poteau and F. Spiegelmann, *J. Chem. Phys.* **98**, (1993) 6540.
16. W.D. Schöne, W. Ekardt, and J. M. Pacheco, *Phys. Rev. B* **50**, (1994) 11079.
17. A. Yoshida, T. Dossing, and M. Manninen, *J. Chem. Phys.* **101**, (1994) 3041.
18. B. Montag and P.-G. Reinhard, *Z. Phys. D* **33**, (1995) 265.
19. S. Kümmel, M. Brack, and P.-G. Reinhard, *Phys. Rev. B* **58**, (1998) 1774; S. Kümmel, P.-G. Reinhard, and M. Brack, to appear in *Eur. Phys. J. D* **9**.
20. J. P. Perdew and Y. Wang, *Phys. Rev. B* **45**, (1992) 13244.
21. K. K. Verma, J. T. Bahns, A. R. Rajaei-Rizi, W. C. Stwalley, and W. T. Zemke, *J. Chem. Phys.* **78**, (1983) 3599.
22. P.-G. Reinhard, O. Genzken, and M. Brack, *Ann. Phys. (Leipzig)* **51**, (1996) 576.
23. H. Häkkinen and M. Manninen, *Phys. Rev. B* **52**, (1995) 1540.
24. Private communication by F. Chandezon and P. Durgourd.
25. J. R. Tessmann, A. H. Kahn, and W. Shockley, *Phys. Rev.* **92**, (1953) 890.
26. C. A. Ullrich, P.-G. Reinhard, and E. Suraud, *J. Phys. B* **31**, (1998) 1871.
27. S. Bjørnholm, J. Borggreen, O. Echt, K. Hansen, J. Pedersen, and H. D. Rasmussen, *Z. Phys. D* **19**, (1991) 47.
28. P. Durgourd, D. Rayane, R. Antoine, and M. Broyer, *Chem. Phys.* **218**, (1997) 163.
29. Private communication by B. Kieninger.